When is high-dimensional scattering chaos essentially two dimensional? Measuring the product structure of singularities

G. Drótos,[1] C. Jung,[2] and T. Tél[1,3]

[1]*Institute of Theoretical Physics, Eötvös University, Pázmány Péter sétány 1/A, H-1117 Budapest, Hungary*

[2]*Instituto de Ciencias Físicas, Universidad Nacional Autónoma de México, Avenida Universidad sin número,*
Apartado Postal 48-3 Cuernavaca, Morelos, Mexico

[3]*Research Group in Theoretical Physics of the Hungarian Academy of Sciences at Eötvös University, Pázmány Péter sétány 1/A,*
H-1117 Budapest, Hungary

We demonstrate how the area of the enveloping surface of the scattering singularities in a three-degrees-of-freedom (3-dof) system depends on a perturbation parameter controlling the distance from a reducible case. This dependence is monotonic and approximately linear. Therefore it serves as a measure for this distance, which can be extracted from an investigation of the fractal structure. These features are a consequence of the dynamics being governed by normally hyperbolic invariant manifolds. We conclude that typical n-dof chaotic scattering exhibits either structures developing out of a stack of chaotic structures of 2-dof type or hardly any chaotic effects.

PACS number(s): 05.45.−a

I. INTRODUCTION

Chaotic scattering plays an important role in several fields of physics ranging from atomic and molecular processes [1], via optics and fluid dynamics [2,3], to astronomy and cosmology [4,5]. While the mechanisms of scattering chaos in two-degrees-of-freedom (2-dof) Hamiltonian systems are well explored by now, relatively little is known of 3-dof systems or systems with even more degrees of freedom. Therefore it is a natural idea to try to use this knowledge of 2-dof systems as a point of entry into the investigation of the chaos of 3-dof systems and check whether 3-dof systems can be understood as a "stack" of 2-dof systems.

The basic idea is then to start with a 3-dof system having an additional conserved quantity besides the total energy due to some corresponding symmetry. This conserved quantity leads to a foliation of the phase space and also of the domain of the Poincaré map into leaves belonging to fixed values of the conserved quantity. If so, the value of the conserved quantity enters the dynamics as a parameter only and we have a reduction of the 3-dof system into a stack of 2-dof systems where the value of the conserved quantity is the stack parameter. Finally, we break the symmetry and destroy the conserved quantity to arrive at a true 3-dof system. At this point the interesting question is how all the structures in phase space or in the domain of the Poincaré map change under this breaking of the symmetry. The experience with a few examples has shown that amazingly small changes occur up to moderate perturbations and that we must come to rather large perturbations to see a substantial change of the structures. Examples from celestial mechanics and from magnetic dipole scattering were treated in Refs. [6,7], respectively, leading to the formulation of a prototypical model [8] for scattering chaos in 3-dof systems. A common feature of these cases is the presence of so-called normally hyperbolic invariant manifolds (NHIMs) in the phase space. The relevance of such objects to scattering chaos was realized by Wiggins and coworkers [9–11] since the stable and unstable manifolds of NHIMs are dividing surfaces that are able to separate regions in phase space. They are thus proper analogs of stable and unstable manifolds of hyperbolic orbits in two-dimensional phase spaces.

The important structures of chaos in scattering systems are the fractals of singularities in scattering functions which reflect the fractal structure of the chaotic invariant set in the Poincaré map. If the dynamics has a conserved quantity, the stack structure of the phase space and of the Poincaré map implies a product structure of the fractals of the singularities of the scattering functions. When we perturb the system and the symmetry, and the conserved quantity becomes approximate only, this product property of the fractal structure becomes approximate, correspondingly. Then the deviation from the product form of the fractal of singularities should serve as a measure of the deviation of the system from symmetry. The purpose of the present article is to follow this idea and to look for quantitative properties of the fractal which can serve as a measure of the deviation from symmetry.

In this paper we show that the area of the surface covering the scattering singularities in the space of initial conditions is an appropriate quantity for this purpose. We find a monotonic increase of this area with the perturbation parameter. Parameter regions where the increase of the surface area is comparable to the surface of the unperturbed case signify strong deviation from the product structure. It is remarkable that no sudden jump occurs in this function.

For small perturbations we also show that the set of singularities at a fixed value of the previously conserved parameter is topologically similar to that of the unperturbed case when sampling it on an appropriate smooth curved surface, instead of using the constant value of the conserved quantity. This provides clear evidence of the structural stability of the set of singularities. In other words, a 3-dof problem that contains NHIMs and is characterized by a small value of the perturbation parameter is essentially equivalent to the unperturbed problem treated in the sense of a stack.

For illustrative purposes we use a prototypical four-dimensional map introduced in Ref. [8] with a simple form of perturbation whose strength is measured by a parameter A ($0 \leqslant A < 1$) (Sec. II). This approach takes advantage of the

fact that it is a lot simpler to handle maps than systems given by a flow in phase space. Section III exemplifies the stack structure of the unperturbed case and its stability. Strongly perturbed cases are investigated in the next section, where we illustrate that the area of the surface covering the set of singularities can be used as a distance from a product structure of singularities. General final remarks are given in Sec. V.

II. PROTOTYPICAL MAP

For a 3-dof autonomous Hamiltonian system the Poincaré map acts on a four-dimensional domain. Now we use as our example of demonstration the prototypical map of Ref. [8], constructed as an analytical approximation to particle scattering in a channel with an obstacle. This map thus corresponds to a system with one open and two closed degrees of freedom. In such systems we often have the same basic situation: One of the closed degrees of freedom can be chosen to play the role of a clock for the Poincaré map (in the channel problem this is the cylindrical radial degree of freedom which triggers the clock whenever the cylinder radial coordinate goes through a relative maximum). The coupling to the other closed degree of freedom can be changed and can be made arbitrarily weak (in the channel this is the cylindrical angular degree of freedom). For zero coupling, the action of this degree of freedom becomes a conserved quantity.

Our map is thus generic for any system of the following class: There is an open degree of freedom and the divergence to infinity of its configurational coordinate defines the asymptotic region. The second degree of freedom is closed and is strongly coupled to the first degree of freedom. The combination of them provides a chaotic scattering system with two degrees of freedom. The intersection condition of the Poincaré map is given by a particular value of the canonical angle coordinate of the second degree of freedom. There is then another closed degree of freedom which might be weakly coupled (this organizes the stack structure through the conserved action of this degree of freedom; see Sec. III). The physical meaning of any of the three degrees of freedom is absolutely irrelevant. The dynamics of a system with two open and one closed degree of freedom is similar and has almost the same properties. Our model is thus prototypical for scattering systems with one open and two closed degrees of freedom, and essentially different properties can be present for three open degrees of freedom only.

The model map has coordinates (q,p,θ,L), where (q,p) and (θ,L) are canonically conjugate pairs representing the open degree of freedom and the second closed degree of freedom, respectively. In the map enters a potential function $V(q)$, which must fulfill the asymptotic condition that it falls to zero rapidly for $q \to \pm\infty$. The corresponding force function $F(q)$ is given as $F(q) = -dV/dq$. For the numerical example we use $V(q) = -\exp(-q^2)$. The map contains the parameter $L_{\max}$ which can be interpreted as the maximal value of L allowed energetically. The step from preimage coordinates (q_n,p_n,θ_n,L_n) to image coordinates $(q_{n+1},p_{n+1},\theta_{n+1},L_{n+1})$ is defined as a three-step process where the first step is a pure twist: $q' = q_n + p_n/2$, $p' = p_n$, $\theta' = \theta_n + L_n/2$, $L' = L_n$. The second

step is a kick:

$$q'' = q', \tag{1}$$

$$p'' = p' + (L_{\max} - L)[1 + A\cos(\theta')]F(q')$$

$$/[1 + AV(q')\sin(\theta')], \tag{2}$$

$$\theta'' = \theta' - [1 + A\cos(\theta')]V(q'), \tag{3}$$

$$L'' = [L' + L_{\max}AV(q')\sin(\theta')]/[1 + AV(q')\sin(\theta')]. \tag{4}$$

The last step is again a twist: $q_{n+1} = q'' + p''/2$, $p_{n+1} = p''$, $\theta_{n+1} = \theta'' + L''/2$, $L_{n+1} = L''$. As has been shown in Ref. [8], there exists a generating function for this map and the pure existence of the generating function guarantees that the map is symplectic.

In the asymptotic region the functions V and F both approach zero rapidly and asymptotically the map simplifies to the free motion

$$q_{n+1} = q_n + p_n, \tag{5}$$

$$p_{n+1} = p_n, \tag{6}$$

$$\theta_{n+1} = \theta_n + L_n, \tag{7}$$

$$L_{n+1} = L_n. \tag{8}$$

Note that asymptotically p and L both become conserved quantities for any value of the perturbation parameter A.

For $A = 0$ the second step of the map reduces to

$$q'' = q', \tag{9}$$

$$p'' = p' + (L_{\max} - L')F(q'), \tag{10}$$

$$\theta'' = \theta' - V(q'), \tag{11}$$

$$L'' = L'. \tag{12}$$

We see that in this limit the "angular momentum" L becomes a conserved quantity and therefore the domain of the map acquires an invariant foliation into leaves of constant L. The variable L organizes thus the stack structure. The (q,p) map of the unperturbed case shall be called the reduced map.

Since we are interested in a scattering problem, we start with trajectories in the incoming asymptotic region, that is, with large values of the modulus of q and the motion directed toward the interaction region. We are interested in the corresponding final asymptotes along which these trajectories eventually leave again the interaction region. The relations between incoming and outgoing asymptotes are the scattering functions. In order to investigate the scattering functions we first need a convenient scheme to label asymptotes. Since the map acts on a four-dimensional domain, we need four labels to specify any asymptote uniquely. It is certainly convenient to use as two of them the asymptotically conserved coordinates p and L. Note that each asymptotic trajectory steps exactly once into the wedge W_1 defined as $q \in [Q - p, Q]$ and once into the wedge W_2 defined as $q \in [-Q - p, -Q)$, where Q is a large positive number.[1] For an incoming asymptote with a pos-

---

[1]The choice of Q is arbitrary, and, as L is asymptotically conserved, one can make it depend on L. We found that structures can best be visualized with a choice of $Q = Q_0 - C\exp[\alpha(L - L_{\max})]$ with $\alpha = 0.523056$, $C = 0.953584$, and $Q_0 = 5.75$, parameters that are used throughout the paper.

itive (negative) value of p we use the q coordinate of its unique point in W_2 (W_1) as the third asymptotic label. Since this third label plays logically the role of a phase shift between the q motion and the trigger of the clock for the Poincaré map we can define a true angle $\chi = -2\pi(q - Q)/p$ in W_1 or $\chi = -2\pi(q + Q)/p$ in W_2. Similarly, as the label for outgoing asymptotes with a positive (negative) value of p we use the q coordinate of its unique point in W_1 (W_2) or the angle $\chi = 2\pi(q - Q)/p$ in W_1 and $\chi = 2\pi(q + Q)/p$ in W_2. As the fourth label we use the relative phase shift between the q and θ motion given by the reduced angle $\psi = \theta - qL/p$. Note that this quantity is constant under the asymptotic motion. The scattering map S gives $\chi_{out}, p_{out}, \psi_{out}, L_{out}$ as functions of $\chi_{in}, p_{in}, \psi_{in}, L_{in}$.

The map S is singular whenever the initial asymptote lies on the stable manifold of a localized trajectory or, more generally, of a set of all localized unstable trajectories of a chaotic saddle. In the case of topological chaos, these singularities form a fractal in the set of initial asymptotes and this fractal contains all the information on the chaotic saddle, and therefore this information can be extracted from asymptotic observations; for more details see Ref. [8]. Singular initial conditions correspond to trajectories with infinite lifetimes. Since they lie on the stable manifold of the chaotic saddle, in any neighborhood of such points one finds trajectories leading to reflection and transmission. This provides a straightforward numerical method to find these points.

III. THE STACK AND ITS STABILITY

The stack property of scattering singularities is clear in the unperturbed case ($A = 0$). The variable L is then a constant of the motion, and the θ dynamics *decouples* from that of p and q [see Eqs. (9)–(12)]. This defines a two-dimensional scattering map for any fixed L, independent of θ, which we call the reduced map.

For any fixed value of p_{in} that is sufficiently small, we find a Cantor set of singularities in χ_{in} (or q) in some finite interval of L_{in}. Considering the full map, there is a compact region of the ($\chi_{in}, \psi_{in}, L_{in}$) space within which the singularities are localized. Since there is no dependence on ψ in the unperturbed case, the set of singularities can be faithfully represented in the plane (χ_{in}, L_{in}). The result shown in Fig. 1 exhibits the stack property: The full problem is built up from layers (corresponding to constant values of L) within which
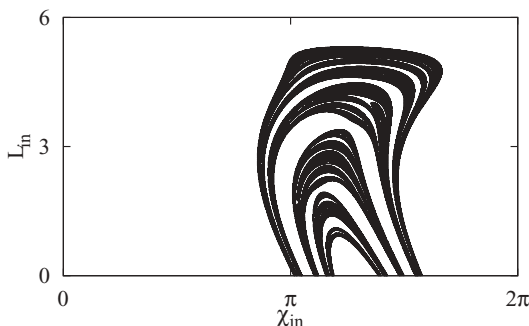

FIG. 1. The stack: singularities of the scattering function in the (χ_{in}, L_{in}) plane for $A = 0$. Different layers in L_{in} are dynamically independent. $p_{in} = -0.5$, $L_{max} = 6$.

the dynamics is independent from that of the neighboring layers.

There is no need to consider different values of p_{in}. As long as $|p_{in}|$ is small enough, any value of it leads to essentially the same fractal (even if for increasing, but still small, values of $|p_{in}|$ some parts of the fractal are dropping out and the optical appearance changes).

The reduced map has its outer fixed points at $q = \pm\infty, p = 0$. The invariant manifolds of these fixed points trace out a ternary symmetric horseshoe. The value $L_{max} = 6$ is chosen such that for $L = 0$ the horseshoe is complete, and this value of L_{max} is used for all numerical examples. With increasing value of L the horseshoe becomes incomplete and runs through the standard development scenario for ternary symmetric horseshoes as described, for example, in Ref. [12]. When L reaches the value L_{max}, the horseshoe reaches development stage 0 and collapses to a parabolic line at $p = 0$. A sequence of plots of this horseshoe for various values of L is shown in Fig. 1 of Ref. [8]. In addition, for increasing values of L the outer tendrils of these horseshoes become shorter and the image of the line of scattering trajectories with $p_{in} = -0.5$ in the domain of the map intersects increasingly smaller parts of these tendrils. Note that fractals are self-similar. Therefore any part of them contains the same information as the complete fractal and also these partial intersections characterize the corresponding horseshoe construction faithfully as long as there is any intersection at all. For approximately $L = 5.33$, the last intersections between the horseshoe and the line of scattering trajectories with $p_{in} = -0.5$ disappear even though the horseshoe itself exists up to $L = L_{max} = 6$. In Fig. 1 these intersection patterns in χ_{in} at a fixed L_{in} have been piled up to give a fractal in the two-dimensional (χ_{in}, L_{in}) plane. This fractal thus encodes the horseshoe development scenario. Note that this fractal consists of an infinite number of smooth curves, including a well-defined outermost (envelope) curve.

Since the chaotic saddle of the reduced two-dimensional map lies in a plane within which the stable and unstable manifolds of the saddle are plane dividing surfaces, and the corresponding manifolds of the full problem are obtained as just a pile of these manifolds, belonging to different L values, the corresponding manifolds of the full problem provide examples of stable and unstable manifolds of *normally hyperbolic invariant manifolds* (NHIMs) [9]. Stable and unstable manifolds of NHIMs play an important role in high-dimensional scattering chaos, being codimension-1 objects, able to separate regions of the full phase space [10,11].

In the unperturbed case, the fractal of singularities in the three-dimensional ($\chi_{in}, \psi_{in}, L_{in}$) space is a Cartesian product of the fractal in the (χ_{in}, L_{in}) plane shown in Fig. 1 with a circle representing the angle ψ_{in} (since the fractal is completely independent of ψ_{in}). Accordingly we need to give only the description of the fractal in the (χ_{in}, L_{in}) plane. It has a natural foliation into a stack of fractals defined along one-dimensional χ_{in} lines for fixed values of L_{in}, where the coordinate L_{in} serves as stack parameter. Moreover, the fractal along the χ_{in} line is just the fractal characterizing the horseshoe of the reduced map for the corresponding value of L_{in}. This construction defines and describes the natural product and stack structure of the fractal in the unperturbed case.
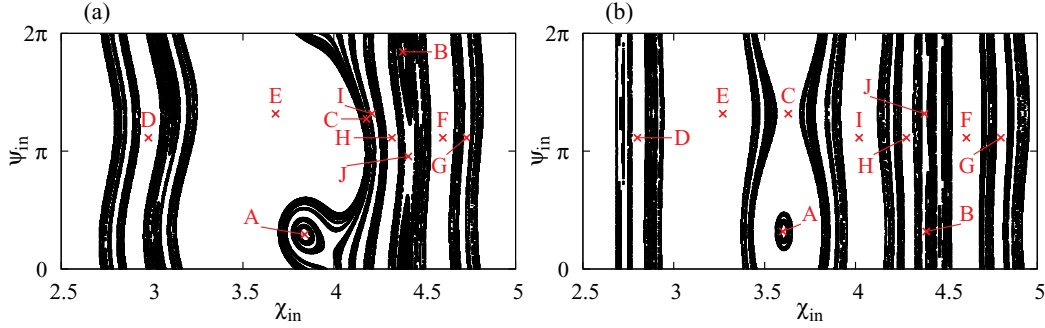
FIG. 2. (Color online) Singularities of the scattering function (a) in the (χ_{in}, ψ_{in}) section defined by $L_{in} = 3.5$ for $A = 0.02$ and (b) as a function of χ_{in}, ψ_{in} along the cut defined by Eq. (13) in the unperturbed case. $p_{in} = -0.5$, $L_{max} = 6$. Labeled points (red, light gray) have topologically similar surroundings.

Now the question arises of how this stack structure is modified when the perturbation is switched on.[2] The observation is that for small values of A the qualitative structure remains the same to a high level of the hierarchy; the fractal is only deformed continuously. We may imagine that the three-dimensional $(\chi_{in}, \psi_{in}, L_{in})$ space with the fractal contained in it is a rubber block and this block is deformed by the perturbation of the system. When we cut the perturbed block along a plane on which L_{in} is *constant,* then the resulting picture looks different from the corresponding picture without perturbation. As a numerical example, see in Fig. 2(a) the cut $L_{in} = 3.5$ with perturbation parameter $A = 0.02$. If the robustness of the stack is true, then it should be possible to obtain a qualitatively similar plot by cutting the block for $A = 0$ along an appropriate *curved* surface, which undoes the continuous deformation. By trial and error we found that the particular example shown in Fig. 2(a) can be approximated

―――――――

[2]Note that the statement on the arbitrary choice of p_{in} is independent of the value of L_{in} for the reduced map; therefore, it holds for the piling of the stack and remains valid also in the presence of a small perturbation.

quite well [see Fig. 2(b)] by a cut on the surface given as

$$L_{in}(\chi_{in}, \psi_{in}) = 3.185 - 0.04 \cos(\psi_{in} - 1.0)$$
$$+ 0.55(\chi_{in} - 3.68). \quad (13)$$

This equation is applied in a strip containing the fractal (outside it should be continued in some form, making it periodic in χ_{in} with period 2π). In the two plots we see a 1:1 correspondence between equivalent structures. To make the comparison easier for the reader, we have marked some points with topologically similar surroundings in the two plots. By choosing a more complicated curved surface we could make the similarity between the two plots even stronger. It is important that one of the fractals can be considered a continuous deformation of the other one. A similar equivalence can be found for any other cut along any plane L_{in} = constant of the perturbed system for small values of the perturbation parameter. This observation is the numerical confirmation of the robustness of the stack property of the system.

When the perturbation parameter is increased, the fractal is deformed more strongly, and in addition, beginning on high levels of the hierarchy, essential changes of the structure come in and the stack property fades out with increasing value of
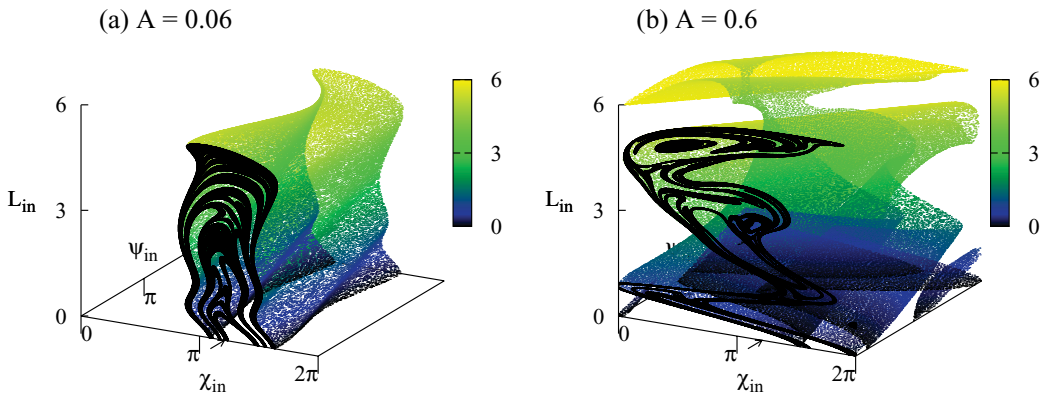

FIG. 3. (Color online) The envelope of the structure of singularities (colored [or gray-scale] surface, where coloring [or brightness] corresponds to the L_{in} values) in the three-dimensional domain (defined by p_{in} = constant) of the scattering function. The detailed structure of singularities is shown on the front section, $\psi_{in} = 0$ (black). The arrow at $\chi_{in} = 3.8$ corresponds to the χ_{in} value defining the section taken in Fig. 4. The value of A is indicated in the panels. $p_{in} = -0.5$ and $L_{max} = 6$.
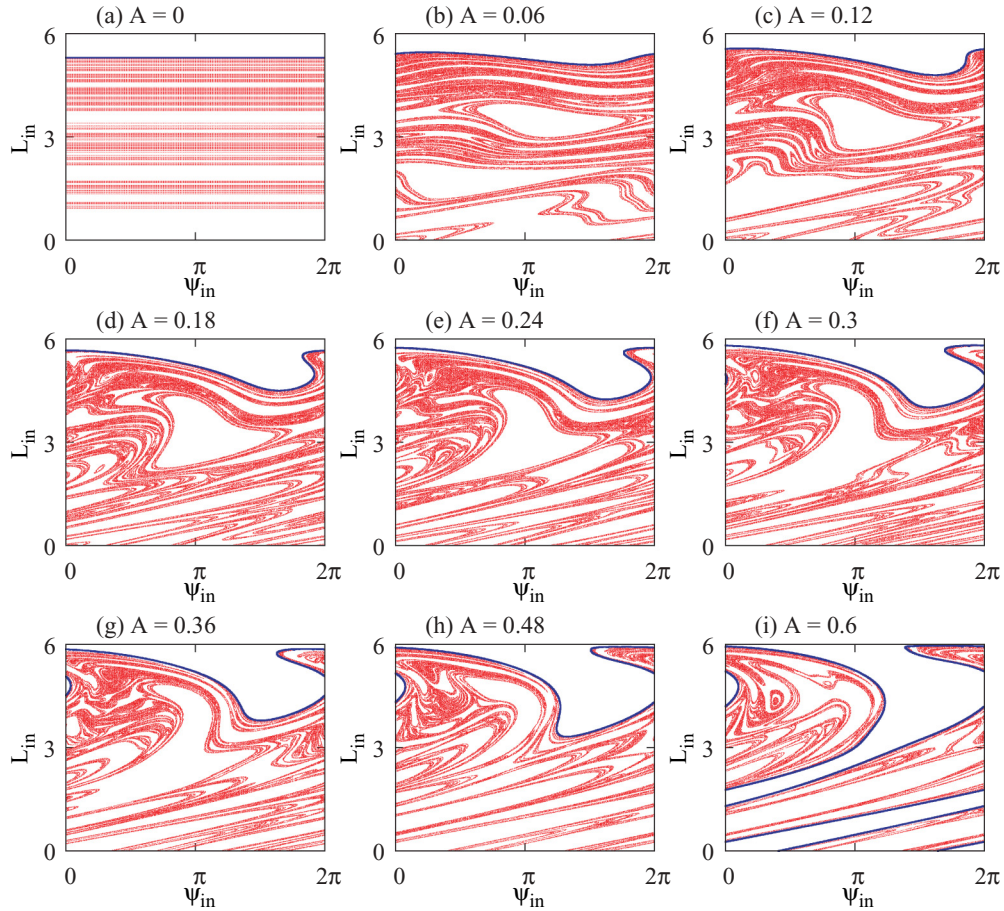
FIG. 4. (Color online) Singularities (red, light gray) of the scattering function in the (ψ_{in}, L_{in}) section defined by $\chi_{in} = 3.8$. The envelope of the structure of singularities is marked by a blue (dark-gray) thick curve. The value of A is indicated in the panels. $p_{in} = -0.5$, $L_{max} = 6$.

A. In the next section we quantify the overall changes of the fractal with increasing A.

IV. STRONG PERTURBATIONS

We investigate how increasing perturbation results in increasing deviation of the set of singularities from the direct product structure in the three-dimensional space spanned by the initial asymptotic variables χ_{in}, ψ_{in}, and L_{in}. Figure 3 gives an impression on the ψ_{in} dependence of the structure of singularities for moderate and larger values of A by plotting the envelope surface of the structure. The difference is striking. In the unperturbed case ($A = 0$), the envelope surface is the product of the outermost curve shown in Fig. 1 with a circle in the variable ψ_{in} and is therefore trivially smooth. Figure 3(a) shows a case when the original direct product structure can still be recognized, while in Fig. 3(b) one can observe a totally deformed surface.

It is difficult, however, to get a detailed impression of such structures in three dimensions, and we thus start with investigating sections of the three-dimensional space. In Fig. 4 the singularities of the scattering function are shown in a (ψ_{in}, L_{in}) plane, in which one directly can see an increasing dependence on ψ_{in}, related to an increasing mixing between

different "levels" of L. We also marked the envelope curve of the structure of singularities in the particular section. The length of this curve exhibits considerable growth with increasing A. This leads to the idea of applying a measure of the envelope to quantitatively characterize the distance from the unperturbed case. The sequence of Fig. 4 illustrates that there is a gradual change in the foliation structure with increasing A, without any jump. Similar behavior is expected therefore in the envelope as well.

There are two main possibilities for characterizing the envelope: On the one hand, we can directly calculate the area a of the envelope surface of the structure embedded in the three-dimensional space of the initial asymptotic variables or, on the other hand, we can approximate it by calculating the lengths l of envelope lines in planar sections of the three-dimensional space. It is practically useful to choose the (χ_{in}, L_{in}) or the (ψ_{in}, L_{in}) planes. For any choice of the plane, averaging is needed over different values of the variable defining the particular section. Multiplying the resulting average length (denoted by $\bar{l}$) by 2π, we obtain an approximation of the area a of the envelope surface.

We emphasize that the exact product and stack property of the whole fractal exhibited in the unperturbed case (discussed in detail in Sec. III) implies the exact product (in direction
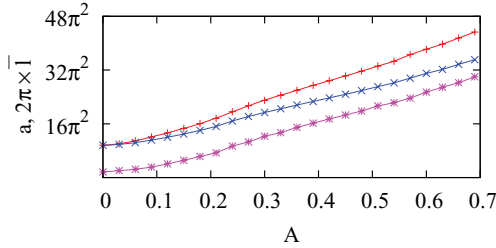
FIG. 5. (Color online) Red line with "+" marks: the area a of the envelope surface of the structure of singularities embedded in the three-dimensional domain of the scattering function (shown in Fig. 3), plotted as a function of parameter A. For comparison, the average envelope length $\bar{l}$ is also plotted (multiplied by 2π), with $\bar{l}$ obtained from (χ_{in}, L_{in}) sections (blue line with "x" marks) and from (ψ_{in}, L_{in}) sections (magenta line with bumped "x" marks) by averaging over 63 values in $[0, 2\pi)$ of variables ψ_{in} and χ_{in}, respectively. $p_{in} = -0.5$, $L_{max} = 6$.

ψ_{in}) and stack (in direction L_{in}) properties of the envelope as well. An increase of the area of the envelope surface without any change in the functional form of the envelope on ψ_{in} or L_{in} could only occur by a pure rescaling induced by the perturbation. However, our Figs. 3 and 4 exclude this option. The observed changes in the functional form of the envelope imply a deviation from the exact applicability of the stack idea. This justifies our expectation that the amount of change of the envelope surface is able to provide an appropriate quantitative measure for the deviation from the exact product and stack properties.

Numerical results on the area of the envelope surface are shown in Fig. 5. The area of the envelope surface is found to be a monotonic function of the perturbation parameter A.[3] Monotonicity is exhibited by both the exact and the approximate methods. All functions are approximately linear. One can also see that the approximation based on the (ψ_{in}, L_{in})

—————

[3]The fractal dimension of the set of singularities is also a natural candidate for being a measure of the deviation from the product structure. Our numerical studies, however, indicate a nonmonotonic dependence of the box-counting dimension on A.

planes gives the correct increment as a function of A, which is not true for the (χ_{in}, L_{in}) planes. It is easy to understand why the cut involving variable ψ_{in} is the more appropriate one. The perturbation parameter A controls to which extent the variable ψ is involved in the dynamics. Consider any cut of the $(\chi_{in}, \psi_{in}, L_{in})$ domain that is not parallel to the $\psi_{in} = $ constant surfaces. The length of the envelope for going around the ψ_{in} circle is the relevant measure of deviation, after averaging or integrating this length over the variable defining the position of the cut (this is simply χ_{in} in our particular choice). The value of the area a is, however, better approximated when using the (χ_{in}, L_{in}) planes. [Note that the (χ_{in}, L_{in}) planes give an exact result for the unperturbed case since all information is contained in one such plane.]

It is worth mentioning that we numerically found initial conditions lying outside the envelope to correspond to trajectories that pass through the scattering region without any turn, even in the perturbed case. This is shown in Fig. 6. This gives the envelope a dynamical meaning and can be explained as follows. First let us consider the reduced map. The outgoing asymptotes χ_{out} and p_{out} are continuous functions of the initial conditions in regions of the two-dimensional domain (χ_{in}, p_{in}) that are bounded by singular initial conditions. One such region of continuity is the one that lies outside the envelope curve (defined as the union of envelope points corresponding to $p_{in} = $ constant sections). In this region one may choose such a large value for $|p_{in}|$ that the corresponding trajectory passes through the scattering region without any turn, irrespective of χ_{in}. Then the outgoing asymptote p_{out} takes some finite value. Any trajectory containing at least one turn could only exist in the same region of continuity if there were initial conditions leading to $p_{out} = 0$ in this region. But $p_{out} = 0$ is only obtained for initial conditions lying on the stable manifold of one of the NHIMs sitting at infinity and being of course singular. Therefore, there is no possibility for the existence of trajectories with any turn in the outer region of continuity. On the contrary, we find reflected trajectories (with an odd number of turns) arbitrarily close to the envelope on the other side of the envelope since envelope points are singular by definition. The set of initial conditions corresponding to a particular $p_{in} = $ constant line is simply obtained by a section of the domain (χ_{in}, p_{in}). These considerations are valid for an arbitrary value of L_{in} for the reduced map so that they
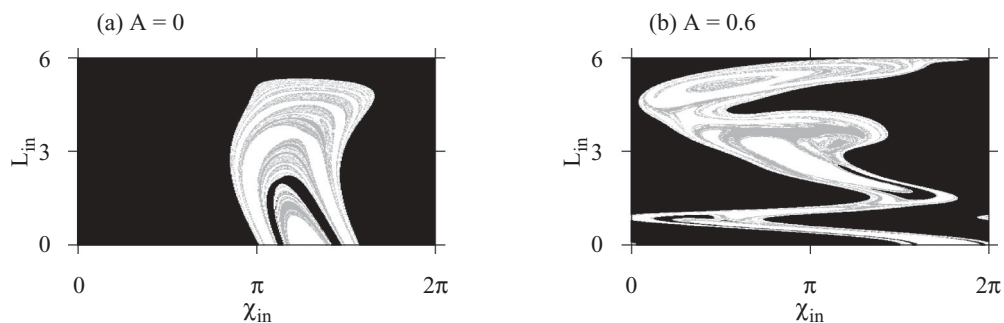

FIG. 6. Turning properties of the trajectories initiated in the (χ_{in}, L_{in}) plane for $\psi_{in} = 0$. Black color indicates that the trajectory passes through the scattering region without any turn, gray color corresponds to transmission with at least two turns of the trajectory, and white color denotes reflection. The value of A is indicated in the panels. $p_{in} = -0.5$, $L_{max} = 6$.

also hold for the unperturbed pile of the stack. As long as a perturbation leads to a smooth deformation of the envelope surface these considerations remain valid. In our particular model this property is enforced by the asymptotic position of the NHIMs as discussed in the next section.

V. DISCUSSION

The Poincaré map for an n-dof autonomous Hamiltonian system acts on a $(2n - 2)$-dimensional domain. In order to be useful as dividing surface (separatrix surface) a surface must be of codimension 1. If this dividing surface should be constructed as a stable or unstable manifold of some invariant subset I of the map, then this subset I must be of codimension 2. It has one transverse stable direction and one transverse unstable direction and the instability associated with any tangential direction should be dominated by the instability associated with the transverse unstable direction.[4] This is the basic idea behind any NHIM [9]. As a consequence, at least locally there is a two-dimensional plane containing a hyperbolic structure in which planar chaos of the same type as in 2-dof systems with their two-dimensional Poincaré map is created. When we now pile up all such two-dimensional hyperbolic planes in all the remaining directions, we arrive naturally at the stack. Compare this with the discussion on topology and dimensions in Ref. [13].

For the case with $n - 2$ further conserved quantities besides the total energy, this layering of the domain of the map is even globally exact. It is enforced by the foliation created by the conserved quantities and by the independence on all the corresponding conjugate cyclic angles. The amazing numerical evidence from examples investigated so far [6–8] is that this global layering remains valid under perturbations which destroy the conserved quantities, and rather strong perturbation is needed to break down the global layering. These numerical observations may have the following explanation: In the examples investigated so far the NHIM itself is persistent for all values of the perturbation and this provides stability properties also for the stable and unstable manifolds of the NHIMs and for their homoclinic or heteroclinic tangles. The NHIMs themselves always have the local layering property and this may facilitate the expansion of this layering—at least approximately—over the whole corresponding homoclinic or heteroclinic tangle.

In the prototypical map studied in the present paper, the two outer NHIMs sit at $q = \pm\infty$ and consist of trajectories which do not move in the q direction. The local segments of their stable manifold consist of trajectories going out to infinity monotonically while the velocity converges to zero. The whole stable manifold is the continuation of these local segments under the inverse map. Note that in linear approximation the fixed points at infinity are parabolic, but they are found to be unstable under the inclusion of the non-

linearities and therefore possess stable and unstable manifolds. This consideration shows that the distinction between the linearly unstable and linearly neutral but nonlinearly unstable cases is rather irrelevant, which provides a novel way to interpret the meaning of the stable and unstable manifolds of NHIMs.

As long as the potential $V(q)$ appearing in the map goes to zero from below for $q \rightarrow \pm\infty$, the above properties hold *independently* of the value of the perturbation parameter A. Remember that the perturbation only acts in the interaction region, and thereby the whole chaotic set is clamped between these two NHIMs at $q = \pm\infty$ independent of A. This guarantees the persistence of the phase space dividing surfaces regardless of the perturbation.

Note that a condition for this rather stable layering is having a potential with an asymptotic attractive tail so that there is no point of no return at a finite distance. We have such attractive tails almost always in potentials occurring in atomic and molecular physics. However, the interpretation of the stable manifolds as trajectories going out with velocity zero only holds for systems with closed degrees of freedom which swallow all energy of the system. In this respect, systems with only open degrees of freedom are essentially different. Our model is thus prototypical for systems with at least one closed degree of freedom.

The rather stable layering of the chaotic set has the following interesting consequence. The pattern of homoclinic or heteroclinic tangles is the one created in two-dimensional planes transverse to the NHIM and thereby coincides with the ones found in Poincaré maps of 2-dof systems. In this sense the chaos of n-dof systems is just a pile of 2-dof chaos and no basically new elements enter the picture. Of course, there exist systems with topological chaos but no NHIM. A well-known 3-dof example is the tetrahedron system (with three open degrees of freedom) [14]. In this system the chaotic set in the Poincaré map is completely hyperbolic, that is, its basic elements are hyperbolic fixed points with two-dimensional stable and unstable manifolds. Accordingly the homoclinic or heteroclinic intersection set is a fractal powder of very low dimension. This low dimension implies that there are typically no scattering singularities appearing along one-dimensional curves in the configurational space. In other words, the chaotic set has little effects on the scattering functions; see the discussion in Ref. [14]. If a n-dof ($n > 2$) scattering system has NHIMs and, in addition, fully hyperbolic elements in its chaotic set (like in the tetrahedron scattering), then the effects of the fully hyperbolic part will be hidden by the effects of the NHIMs. Then the final conclusion is that typical n-dof ($n > 2$) chaotic scattering shows either structures developing out of a stack of chaotic structures of 2-dof type or hardly any chaotic effects.

---

[4]Note that in our particular model map the NHIM is located in the asymptotic region, and we thus find *neutral* stability of any point of the NHIM in directions L and θ; see Eqs. (5)–(8). This particular property of our model is irrelevant for the generality of the results.

[1] Z. Kovács and L. Wiesenfeld, Phys. Rev. E **51**, 5476 (1995).
[2] E. G. Altmann, Phys. Rev. A **79**, 013830 (2009).
[3] C. Jung, T. Tél, and E. Ziemniak, Chaos **3**, 555 (1993).
[4] P. T. Boyd and S. L. W. McMillan, Chaos **4**, 507 (1993).
[5] A. E. Motter and P. S. Letelier, Phys. Lett. A **285**, 127 (2001).
[6] L. Benet, J. Broch, O. Merlo, and T. H. Seligman, Phys. Rev. E **71**, 036225 (2005).
[7] F. Gonzalez and C. Jung, J. Phys. A: Math. Theor. **45**, 265102 (2012).
[8] C. Jung, O. Merlo, T. H. Seligman, and W. P. K. Zapfe, N. J. Phys. **12**, 103021 (2010).
[9] S. Wiggins, *Normally Hyperbolic Invariant Manifolds in Dynamical Systems* (Springer, Berlin, 1994).
[10] H. Waalkens, R. Schubert, and S. Wiggins, Nonlinearity **21**, R1 (2008).
[11] H. Waalkens and S. Wiggins, Regul. Chaotic Dyn. **15**, 1 (2010).
[12] C. Jung, C. Lipp, and T. H. Seligman, Ann. Phys. **275**, 151 (1999).
[13] Z. Kovács and L. Wiesenfeld, Phys. Rev. E **63**, 056207 (2001).
[14] Q. Chen, M. Ding, and E. Ott, Phys. Lett. A **145**, 93 (1990).